FRACTAL PHASE DISTRIBUTION AND DRYING: IMPACT ON TWO-PHASE ZONE SCALING AND DRYING TIME SCALE DEPENDENCE

Marc Prat[1], Stéphanie Veran-Tissoires[1],Nicole Vorhauer[2], Thomas Metzger[2], Evangelos Tsotsas[2]

[1]INPT, UPS, IMFT (Institut de Mécanique des Fluides de Toulouse), Université de Toulouse, Allée Camille Soula, F-31400 Toulouse, France and CNRS, IMFT, F-31400 Toulouse, France

[2]Thermal Process Engineering, Otto von Guericke University
Universitaetsplatz 2, 39106 Magdeburg, Germany

[*]e-mail : mprat@imft.fr

In an article published in 2008[1], Professor A.R. Mujumdar and his colleagues reviewed some applications of fractal concept on drying. As a modest continuation to this article, we give an overview on three drying related issues where fractal aspects are present. First, we discuss within the framework of the theory of invasion percolation in a gradient the characteristic lengths that determine the extent of the hydraulically connected region during drying. It is pointed out that the scaling of this region is fundamentally different in 2D and in 3D owing to the different percolation properties in 2D and 3D. In particular, it is shown that the fractal region only represents a small region of a drying front in 3D systems. Then a situation is described where fractal porous structures form as a result of an evaporation process. Finally we consider drying in systems characterized by an initial fractal distribution of the liquid phase (invasion percolation cluster), a situation expected to happen in PEM fuel cells, and explore the size dependent property of the overall drying time from pore network simulations.

INTRODUCTION

The introduction of fractal concepts in relation with the characterization of porous media and the study of transport phenomena in porous media dates back to the eighties which were the golden age as regards the spreading of fractal concepts in physics and chemistry in general. The literature of those years is abundant and one can refer to different books [2-4] for overviews of the field. About 25 years after the hype of the eighties, the use of fractal concepts in relation with porous media studies is much more moderate. Nevertheless, fractal concepts remain an interesting tool everyone should know. Since a nice review in relation with drying problems is available in [1], the idea is rather here to discuss only three aspects of drying and evaporation where fractal concepts are important or present. The fist one is the concept of length scale associated with the two-phase zone that forms in drying as a result of evaporation under classical conditions. This length scale is important to predict and can be analyzed for example from drying simulations after the fast drying rate period has ended. The second one is related to porous structures, which can be fractal like as the result of an evaporation process. The third one is related to the structure of the liquid distribution at the beginning of drying, which can also be fractal like.

[*] Correspondence : Marc Prat, Institut de Mécanique des Fluides de Toulouse, Avenue du Professeur Camille Soula, 31400 Toulouse, France ; E-mail : mprat@imft.fr

CHARACTERISTIC LENGTHS IN DRYING

We consider the basic drying situation depicted in Fig.1. Evaporation, at ambient temperature, of a liquid initially saturating a rigid porous medium of height H results from the gas convection along its upper, horizontal, free surface or in the absence of convection from the vapour diffusion in the surrounding dryer air. The other boundaries of the porous medium are in contact with approximately isothermal, rigid, impermeable surfaces. The temperature of the external gas remains close to the ambient temperature so that temperature gradients are negligible during the drying experiment. We consider the classical case of capillary porous media in which hygroscopic effects (i.e. the adsorption of liquid on pore walls) can be neglected. The drying curve for this type of material under these drying conditions is classically described in three main periods as follows [5]. During the first period, referred to as the CRP (constant rate period), the evaporation rate is essentially constant and controlled by the external demand (velocity and relative humidity in surrounding air). The last period, the receding front period (RFP), is characterized by an internal evaporation front receding into the porous medium whereas the intermediate period, the falling rate period (FRP), is a crossover period characterized by a significant drop in the drying rate. When the mass loss δm of the sample due to evaporation is plotted as a function of time, one generally obtains curves similar to the one shown in Fig.2, which illustrates the very significant decrease in the drying rate equal to $-\frac{d(\delta m)}{dt}$ after the CRP. A key issue in the drying theory is to predict the drying curve. Here we will simply discuss the prediction of the extent of the CRP, by determining the end of this period which marks the beginning of the RFP if one neglects the short intermediate FRP. We consider that the CRP ends when the porous medium surface ceases to be hydraulically connected to the liquid present inside the porous medium. In the classical description of the drying curve, this definition rather corresponds to the end of the FRP. However, the FRP is often short compared to the two other periods and therefore it is often not important to clearly distinguish the time marking the end of CRP from the time marking the end of FRP. In other terms, we consider in fact that it is sufficient to distinguish two main drying periods (as shown in Fig.2): the CRP/FRP period referred to as the first drying period in this paper, and the receding front period, referred to as the second drying period in this paper. The fact that the first period ends when a dry zone begins to form in the top region of the sample is widely admitted[5-7]. There is a problem however as regards the definition of the hydraulic connectivity of the liquid phase. The simplest option is to neglect the possible effect of thick liquid films[8-9] that can be present in the corners of non-cylindrical pores, crevices of the pore space or the roughness of the pore walls. Under these circumstances, the term *hydraulically connected to the surface* means that there exist surface pores fully occupied by liquid and connected to the liquid pores deeper inside the sample by a path of fully saturated liquid pores. This is the situation considered for example in the first generation of pore network models, i.e. [10], [11] and references therein. As shown with the simple drying experiment for a single tube of square cross section reported in [9], the thick films can however provide hydraulic paths to transport the liquid up to the surface even in the absence of fully saturated pores at the surface. As discussed in several previous works[8,12-15] and depicted in Fig.1, one can therefore distinguish in fact four main zones in terms of phase distribution when the RFP is reached: a fully saturated zone adjacent to the sample bottom, a two-phase zone where pores fully occupied by the liquid and pores invaded by the gas phase coexist, a dry zone adjacent to the top surface of the sample and a film region between the top of the two-phase zone and the dry zone. Films are of course also present in pores occupied by the gas phase in the two-phase zone. According to this picture, which has not yet been completely confirmed for "real" porous media, the extent L of the hydraulically connected zone (the saturated zone is not considered) is therefore,

$$L = L_{tp} + L_f \tag{1}$$

where, as depicted in Fig.1, L_{tp} and L_f are the vertical extent of two-phase zone and pure film region, respectively. The extent of the film region roughly decreases with mean pore size owing to viscous effects and as a result strong film effects have been demonstrated so far only for relatively coarse porous media. Also, one can notice that the evaporation rates typical of convective drying in industrial applications are usually greater than the ones measured in a laboratory experiment at room temperature. This is another factor limiting the extent of liquid films in applications. As a result, throughout this paper we will make the assumption that $L_f << L_{tp}$. From Eq.(1), we therefore consider that $L \approx L_{tp}$. That means that the first drying period ends when the position, measured from the porous medium surface, of the most advanced points of the two-phase zone in the porous medium is of order L_{tp}. The next step is to predict L_{tp}.

Although an approximate and useful approach based on classical concepts has been proposed for 3D systems in [7], the theoretical framework convenient to discuss the length scale L_{tp} both for 2D and 3D systems is the theory of invasion percolation in a gradient, e.g. [11], [12] and references therein. From previous works, see [11], [12], we know that the extent of the two phase zone depends on the competition between capillary effects, viscous effects (in the liquid phase) and gravity effects. As illustrated in Fig.3 from pore network simulations[16], both gravity and viscous effects are stabilizing and therefore contribute to the formation of a two phase zone of limited length within the porous sample. Following previous works, e.g. [17], [18], the two-phase zone extent L_{tp} is defined as the distance between the most advanced point and the least advanced one of the two phase zone. In two dimensional systems, the length L_{tp} can be expressed as

$$L_{tp} = \lambda \left(\frac{B}{\Sigma} \right)^{-1+\frac{1+\beta}{1+\nu}} \tag{2}$$

when the length of the two-phase zone is dominated by the competition between capillary and gravity effects. In Eq.(2), λ is a numerical pre-factor, B is the bond number ($B = \dfrac{\rho_\ell g \bar{r}}{\gamma \cos\theta}$ where ρ_ℓ is the liquid density, g the gravity acceleration, γ the surface tension, θ the wetting angle and $\bar{r}$ is an average pore size); $\Sigma = \dfrac{r_{\max} - r_{\min}}{\bar{r}}$ is a measure of the width of the pore size distribution; β and ν are the percolation probability and the correlation length exponents of the percolation theory[19]; β = 5/36 and ν = 4/3 in a 2D system, which leads to $-1+\dfrac{1+\beta}{1+\nu} = -0.52$. In this 2D case, the two-phase zone is essentially formed by a travelling fractal front with some isolated liquid clusters in the "fjords" of the front (see Fig.1). When the viscous forces are responsible for the limited extent of the two-phase zone, the length L_{tp} is expected to read[17],

$$L_{tp} = \lambda_v \left(\frac{Ca}{\Sigma} \right)^{-1+\frac{1+\beta}{1+\nu}} \tag{3}$$

where the capillary number, characterizing the competition between capillary and viscous effects, is given by $Ca = \frac{e\mu_\ell}{\gamma \wp_\ell}$, where e is the evaporation flux (constant in the first drying period and computed from the external transfer conditions) and μ_ℓ the liquid dynamic viscosity. It is worth noticing that Eq.(3) is fully consistent with the sole available experimental results[18], but that more accurate results from experiments or pore-network simulations for example are still desirable to better confirm Eq.(3). Fractal concepts are therefore central to determine the length L_{tp} in two dimensional systems (this is because the 2D invasion front operates near the percolation threshold of the porous microstructure and it is well known that a percolation cluster is a fractal object, see [20] for more details). Owing to the greater connectivity of the pore space, the situation is quite different in a 3D porous structure. The two-phase zone in 3D systems was first discussed in [21] and further details can be found in [22] and [23]. The essential difference is that the fractal region (near the percolation threshold of the network) is confined to a small region in the most advanced region of the two-phase zone. As sketched in Fig.4, the profile is characterized by two regions: a short frontal region of size σ and a much larger compact region of size ξ. Hence $L_{tp} \approx \xi+\sigma$. For the gravity stabilized case, the scaling law governing the size ξ reads

$$\xi \sim \left(\frac{B}{\Sigma}\right)^{-1} \tag{3}$$

whereas the size of the frontal region varies as,

$$\sigma \propto \left(\frac{B}{\Sigma}\right)^{-\frac{\nu}{1+\nu}} \tag{4}$$

which gives $\sigma \approx \left(\frac{B}{\Sigma}\right)^{-0.47}$ using the known value of the correlation exponent for 3D systems ($\nu = 0.88$[19]). Similarly, the scaling of the compact region is $\xi \sim \left(\frac{Ca}{\Sigma}\right)^{-1}$ when viscous effects are responsible for the stabilizing effect whereas $\sigma \propto \left(\frac{Ca}{\Sigma}\right)^{-\frac{\nu}{1+\nu}}$ as discussed in more details in [24]. Because of the significantly lower exponent for the frontal region, the frontal region is generally much smaller than the compact region and in fact usually negligible under practical conditions. The scaling of the compact region is fully consistent with the classical continuum approach to drying, e.g. [25], and this explains why the characteristic length of the two-phase region can be deduced from usual macroscopic concepts in the case of 3D systems, e.g. [7].
The above discussion applies to situations where $L_{tp} < H$. When $L_{tp} \geq H$, the situation is of course different since the two-phase zone can extend over the full height of the sample. This corresponds to the capillary regime discussed in [11] and the end of the first drying period in 3D systems can be estimated in this case using an approach similar to the one developed in [6].

FRACTAL SALT STRUCTURES GENERATED BY AN EVAPORATION PROCESS

An interesting and yet relatively little explored problem is the formation of efflorescence at the surface of a porous medium[26] Salt crystallization can be a problem in relation with the underground sequestration of CO_2 [27] and is an important issue in building physics because of

the severe damages caused by the crystallization process[28]. Salts can enter stone and masonry by several routes, the simplest of which is the capillary rise of groundwater. As the water penetrates a wall, it also evaporates. When the evaporation front is within the porous medium, salt crystals will precipitate inside the porous medium if the solution becomes supersaturated; this is called *subflorescence.* When the liquid/vapor interface remains at the porous medium surface, supersaturation leads to precipitation at the surface or *efflorescence*. Although less damaging than subflorescence, efflorescence is an important issue for the conservation of old paintings and frescoes. Fig.5 shows two examples of efflorescence obtained from the evaporation of a NaCl aqueous solution. The first one was formed at the surface of saturated porous medium[29] whereas the second one developed on a glass plate partially immersed in the salt solution. As shown in [30], efflorescence can form fractal structure and this is qualitatively illustrated in Fig.5b which shows a structure resembling classical DLA (Diffusion Limited Aggregation) structures[31]. Figure 5a shows, however, that more compact structures can be obtained as well. In fact, as in many non-equilibrium growth processes[31], the efflorescence structures can be more or less ramified depending on the formation conditions (evaporation rate, temperature, presence of impurities, etc). A lot of work remains to be done to characterize the efflorescence growth process, which is only qualitatively understood. As discussed in [32] and illustrated in Fig.5b, efflorescence structures are porous and therefore hydraulically connected to the liquid solution located at its bottom or traveling in the underlying porous medium. The efflorescence grows owing to the salt deposition occurring preferentially in the upper region of efflorescence where evaporation is higher. The problem can be seen as the one of a Laplacian field (the vapour concentration field around the efflorescence is essentially controlled by diffusion at the scale of the efflorescence) with an irregular boundary (the efflorescence). This qualitatively explains why structures typical of Laplacian growth[31] are obtained here. Further details on this interesting and widely open problem can be found in [26], [29] and [30].

DRYING WITH INITIAL FRACTAL LIQUID DISTRIBUTIONS

Another situation where a fractal structure is encountered in a drying problem is found when the liquid phase forms a fractal distribution at the beginning of drying. We consider a hydrophobic system; i.e. a system in which the contact angle of the water with the pore walls is sufficiently greater than 90° (why “sufficiently” greater and not “exactly” greater than 90° is explained in [33]). Typical practical examples are “teflonized” materials, i.e. materials that have been treated so that the pore wall is carpeted by PTFE (Polytetrafluoroethylene or Teflon). The advancing contact angle of water on PTFE is on the order of 110°-120°. PTFE or other hydrophobic agents are for example used to render the stones of buildings and monuments hydrophobic in order to prevent damages associated with the capillary rise of groundwater[28]. Another example intensively studied in recent years is the so-called gas diffusion layer (GDL) of proton exchange membrane fuel cells (PEMFC), e.g. [34]. As a result of electrochemical reactions, liquid water can invade the hydrophobic GDL, which can be detrimental to the fuel cell operation. At some stages in the operation of the fuel cell, it can be desirable to get rid of the water by drying the GDL. As discussed in some details in [35] and [36], water invasion in the GDL is a capillarity controlled invasion process, which leads to fractal water distributions (an invasion percolation cluster) as a result of the hydrophobic nature of the medium. An example of invasion percolation in a two-dimensional network is shown in Fig.6. To get some preliminary insights into this drying situation, that is the drying of a medium in which the initial distribution of the liquid forms a percolation cluster, we have performed the following pore network simulation study. We consider a two-dimensional $N \times N$ square network. In a first phase, water invasion is simulated using the classical invasion percolation algorithm[37] up to breakthrough (water is injected from the bottom and the

simulation is stopped as soon as water has reached the top edge of the network). This typically leads to invasion patterns similar to the one shown in Fig.6. Then, drying of the network is computed using the classical pore network model proposed in [38]. In fact, using this model can be questioned since the medium considered is hydrophobic. As discussed in detail in [33] and [39], the simulation of drying in a hydrophobic network can be much more involved than simulation of drying in a hydrophilic medium because of cooperative effects between adjacent menisci during drying. However, it has been shown that the receding contact angle of water on a Teflon surface can be significantly lower than the advancing contact angle. Values as low as 80° have been reported[40]. Due to this the medium can be considered in fact as hydrophilic as one regards the drying problem. This justifies the use of the classical pore network model of drying. For the sake of brevity and since this model is described in several previous papers[11,15,38], we will not describe it here again. For simplicity, we assume that the pore network is open at the top whereas the other edges are in contact with impervious boundaries. At the top, we assume that the external resistance to mass transfer is very small so as to focus on the effect of the internal mass transfer resistance. We have computed the overall drying time of the network as a function of network size. For each size considered, many realizations of the network have been generated and the results are thus expressed in terms of average drying time over the number of realizations considered (see caption of Fig.7 for more details). Owing to the fractal nature of the initial liquid distribution (an invasion percolation cluster as explained before), it is expected that the drying time exhibits some scale dependence. As illustrated in the inset of Fig.7, the initial mass of liquid in the network follows a non-trivial power law, $M_0 \propto L^d$. A best fit of our data gives $d = 1.82$, in very good agreement with the known value of this exponent[19]. As can be seen from Fig.7, the average drying time $<\tau>$ can be also expressed according to a power law as,

$$<\tau> = \lambda_\tau L^b \tag{5}$$

where λ_τ is a numerical pre-factor. A best fit from the data reported in Fig.7 yields for the exponent $b \approx 1.88$. This behaviour is significantly different from the one obtained starting from a fully saturated network, see [39], which leads to an exponent slightly greater than 2 owing to an effect which has nothing to do with fractal concepts (see [39] for more details). It can thus be concluded from these preliminary simulations that an initial fractal distribution of the liquid leads to a non-trivial variation of drying time with system size.

CONCLUSIONS

In this article, we have discussed a few aspects of drying and evaporation where fractal concepts are important or useful. We have seen that the fractal concepts are essential to determine the characteristic length of the two-phase zone (regardless of film effects that can lead to a wider two-phase zone) resulting from drying in two-dimensional systems whereas the fractal two-phase region can generally be neglected in three-dimensional systems. As mentioned in the article, the concept of characteristic length scale is useful to determine the transition between different drying periods. It is therefore important to clearly understand the fundamental differences between two-dimensional and three-dimensional systems.

Then we have briefly discussed a situation where an evaporation process leads to the formation of fractal-like structures with the example of salt efflorescence. Interestingly, some advances in the phenomenology of efflorescence formation and growth have been made recently, e.g. [26], but the quantitative characterization is yet a quite open problem.

Finally, we have shown that fractal aspects can come from the initial distribution of the liquid, when, as considered in this article, the phase distribution results from an invasion percolation process.

Although fractal concepts are certainly much less fashionable than in the eighties, they should undoubtedly have a place in the tool box of drying practitioners.

REFERENCES

1. Xu, P., Mujumdar, A.R., Yu, B. Fractal theory on drying : a review, *Drying Technology* **2008**, *26*, 640-650.
2. Bunde, A., Havlin, S. (Eds). *Fractal and disordered systems*, Springer Verlag: Berlin – Heidelberg, **1991**.
3. Avnir, D. (Ed.). *The fractal approach to heterogeneous chemistry*, John Wiley: New-York, **1983**.
4. Sahimi, M. *Flow and transport in porous media and fractured rock*, VCH Weinheim, **1995**.
5. Van Brakel, J. Mass transfer in convective drying, in Advances in Drying, A.S. Mujumdar ed., Hemisphere: New-York, pp. 217- 267 ,1980.
6. Coussot, P. Scaling approach to the convective drying of a porous medium, *Eur. Phys. J. B* **2000**, *15*, 557 – 566.
7. Lehmann, P., Assouline, S., Or, D. Characteristic length affecting evaporative drying of porous media, *Phys. Rev. E* **2008**, *77*, 056309.
8. Yiotis, A.G., Boudouvis, A.G, Stubos, A.K., Tsimpanogiannis, I.N., Yortsos, Y.C. The effet of liquid films on the isothermal drying of porous media. *Phys. Rev. E* **2003**, 68, 037303.
9. Chauvet, F.; Duru, P.; Geoffroy, S.; Prat, M. Three periods of drying of a single square capillary tube, *Phys. Rev. Lett.* **2009**, 103, 124502.
10. Le Bray, Y.; Prat, M. Three dimensional pore network simulation of drying in capillary porous media, *Int. J. of Heat and Mass Tr.* **1999**,42,4207-4224.
11. Prat, M. Recent advances in pore-scale models for drying of porous media, *Chem. Eng. J.* **2002**, 86 (1-2), 153-164.
12. Yiotis, A.G.; Boudouvis, A.G.; Stubos, A.K.; Tsimpanogiannis, I.N.; Yortsos, Y. The effect of liquid films on the drying of porous media. *AiChE J*. **2004**, 50 (11), 2721-2737.
13. Yiotis, A.G.; Tsimpanogiannis, I.N.; Stubos A.K.; Yortsos,Y. Pore-network study of the characteristic periods in the drying of porous materials, *J. Colloid Interface Science* **2006**, 297, 738-748
14. .Prat, M., On the influence of pore shape, contact angle and film flows on drying of capillary porous media*, Int. J. of Heat and Mass Tr.* **2007***,* 50,1455-1468.
15. Prat, M. Pore network models of drying, contact angle and films flows, *Chem. Eng. Technol.* **2011,** 34 (7), 1029–1038.
16. Metzger, T.; Tsotsas, E. Viscous stabilization of drying front: three-dimensional pore network simulations, *Chemical Engineering Research and Design* **2008**, 86, 739-744
17. Prat, M.; Bouleux, F. Drying of capillary porous media with stabilized front in two-dimensions. *Phys. Rev.E* **1999,** 60, 5647-5656.
18. Shaw, T.M., Drying as an immiscible displacement process with fluid counterflow, *Phys. Rev. Lett.* **1987**, 59(15),1671-1674.
19. Stauffer, D.; Aharony A. *Introduction to percolation theory*. Taylor & Francis, London, 1992.
20. Sapoval, B.; Rosso,M.; Gouyet, J.F. The fractal nature of a diffusion front and the relation to percolation, *J.Phys. Lett.* **1985**, 46, 149-156.
21. Gouyet, J.F.; Rosso M.; Sapoval, B.. Fractal structure of diffusion and invasion fronts in three-dimensional lattices through the gradient percolation approach. *Phys. Rev. B* **1988***,* 37, 4, 1832-1838.

22. Xu B.; Yortsos Y.; Salin D. Invasion percolation with viscous forces. *Phys. Rev. E* **1998,** 57(1):739-751.
23. Yortsos Y.; Xu B.; Salin D. Phase diagram of fully developed drainage in porous media. *Phys. Rev. Lett.* **1997,** 79(23), 4581-4584.
24. Tsimpanogiannis, I.N.; Yortsos, Y.; Poulou, S.; Kanellopoulos, N.; Stubos, A.K. Scaling theory of drying in porous media, *Phys.Rev.E* **1999**, 59, 4, 4353-4365.
25. Whitaker S., Simultaneous heat, mass and momentum transfer in porous media. A theory of drying. Advances in Heat Transfer vol.13, Academic Press, New-York 1977.
26. S.Veran-Tissoires, M.Marcoux, M.Prat, Discrete salt crystallization at the surface of a porous medium, accepted for publication in *Phys.Rev.Letters* **2012.**
27. Peysson, Y.; Bazin, B.; Magnier, C.; Kohler, E.; Youssef, S. Permeability alteration due to salt precipitation driven by drying in the context of CO_2 injection, Energy Procedia **2011,** 4, 4387–4394.
28. Scherer, G.W.; Flatt, R.; Wheeler, G. Materials Science Research for the Conservation of Sculpture and Monuments, MRS Bulletin **2001** (January), 44-50.
29. S.Veran-Tissoires, Ph.D Thesis, Université de Toulouse, 2011.
30. Du, R.; Stone, H.A., Evaporatively controlled growth of salt trees, *Phys.Rev. E.* **1996**, 53, 2, 1994-1997.
31. Meakin, P.: Fractals, scaling and growth far from equilibrium, Cambridge University Press, 1998.
32. Sghaier, N.; Prat, M. Effect of efflorescence formation on drying kinetics of porous media, *Transport in Porous Media* **2009**, 80 (3), 441-454.
33. Chraibi, H.; Prat, M.; Chapuis, O. Influence of contact angle on slow evaporation in two dimensional porous media, *Phys. Rev. E* **2009**, 79, 026313
34. Mukherjee, P.P.; Kang, Q.; Wang, C.Y. Pore-Scale Modeling of Two-Phase Transport in Polymer Electrolyte Fuel Cells - Progress and Perspective, *Energy & Environmental Science – Royal Society of Chemistry* **2011**, 4, 346.
35. Chapuis, O.; Prat, M.; Quintard, M.; Chane-Kane, E.; Guillot, O.; Mayer, N. Two-phase flow and evaporation in model fibrous media. Application to the gas diffusion layer of PEM fuel cells, *J. of Power Sources* **2008** 178, 258 -268.
36. Ceballos, L.; Prat, M.; Duru, P. Slow invasion of a nonwetting fluid from multiple inlet sources in a thin porous layer. *Phys. Rev. E* **2011,** 84, 056311.
37. Wilkinson,D.; Willemsen, J.F. Invasion percolation: a new form of percolation theory, *J.Phys.A:Math.Gen.* **1983,** 16, 3365-3376.
38. Prat, M. Percolation model of drying under isothermal conditions in porous media. *Int. J. of Multiphase Flow* **1993**, Vol.19,No.4, pp.691-704.
39. Chapuis, O.; Prat, M. Influence of wettability conditions on slow evaporation in two-dimensional porous media, *Phys. Rev. E* **2007,** 75**,** 046311.
40. Parry, V.; Berthomé, G. ; Joud, J.C. Wetting properties of gas diffusion layers: application of the Cassie-Baxter and Wenzel equations. Accepted for publication in *Applied Surface Science.*

List of figures

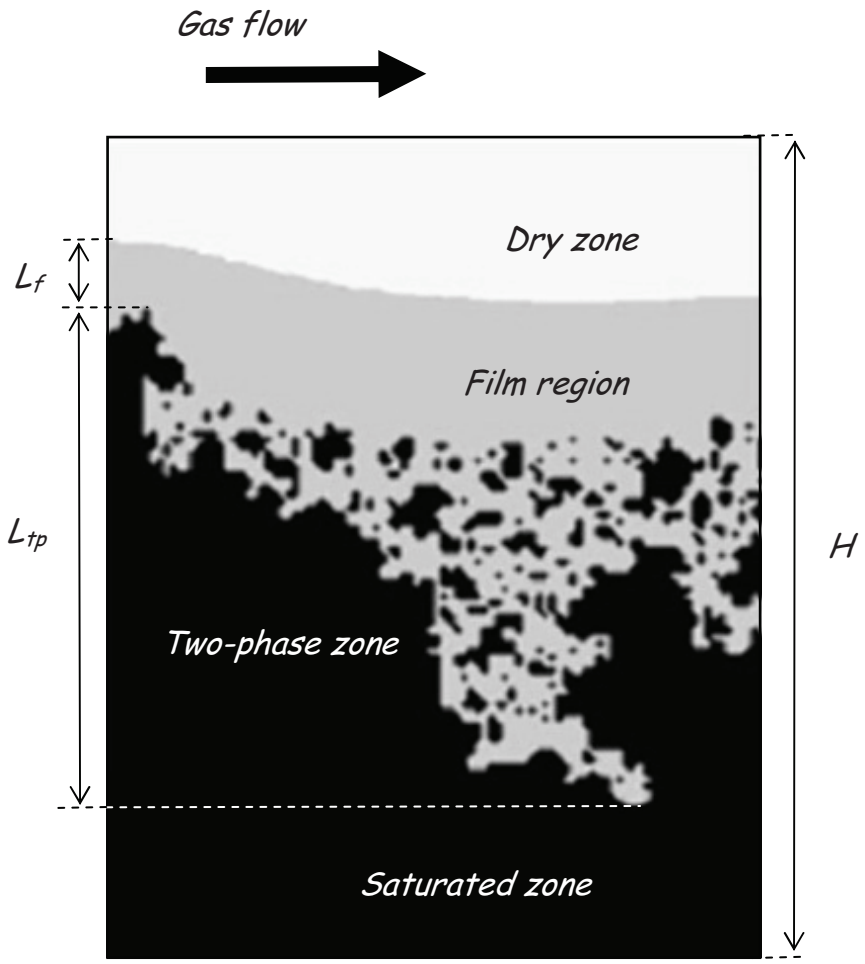
Gas flow
Dry zone
Film region
Two-phase zone
Saturated zone
L_f
L_{tp}
H

Fig.1

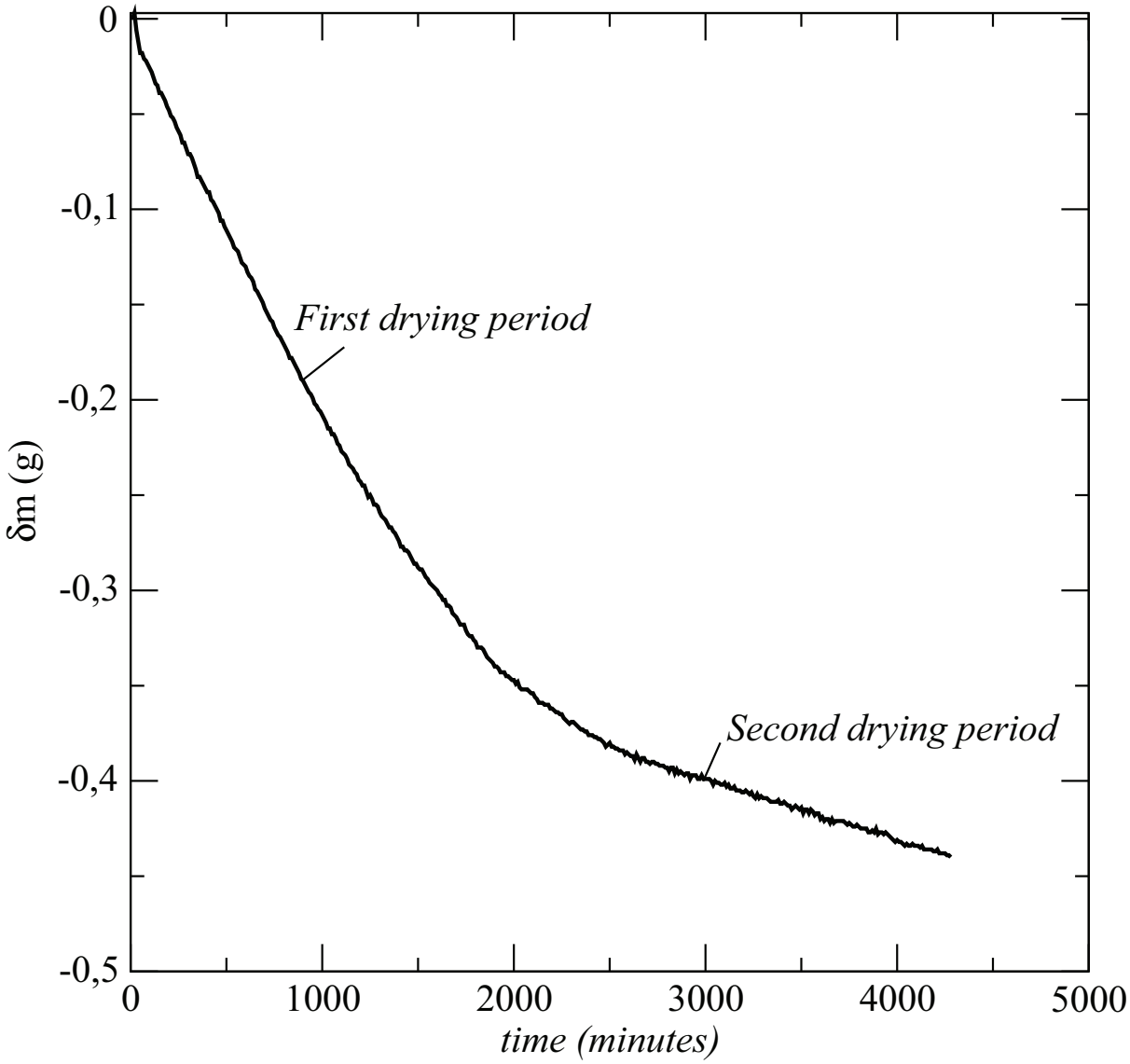
0
-0,1
-0,2
-0,3
-0,4
-0,5
δm (g)
First drying period
Second drying period
0
1000
2000
3000
4000
5000
time (minutes)

Fig.2

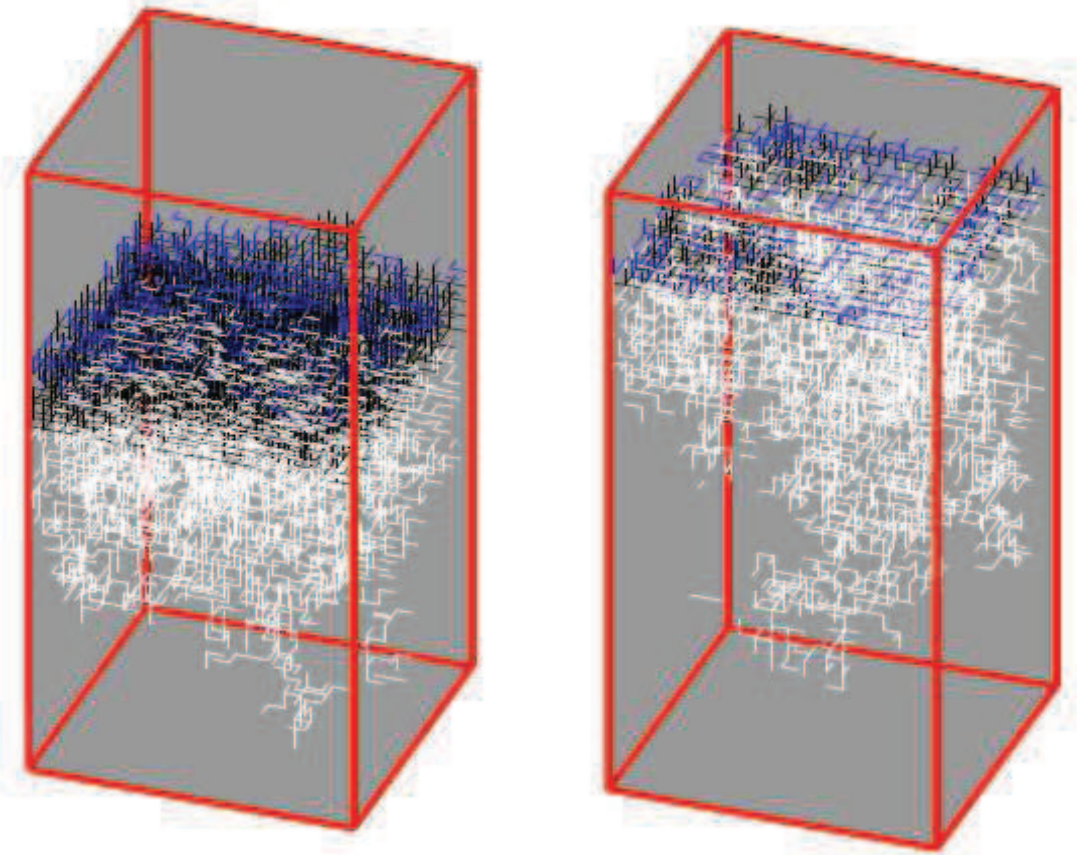

a) b)

Fig. 3.

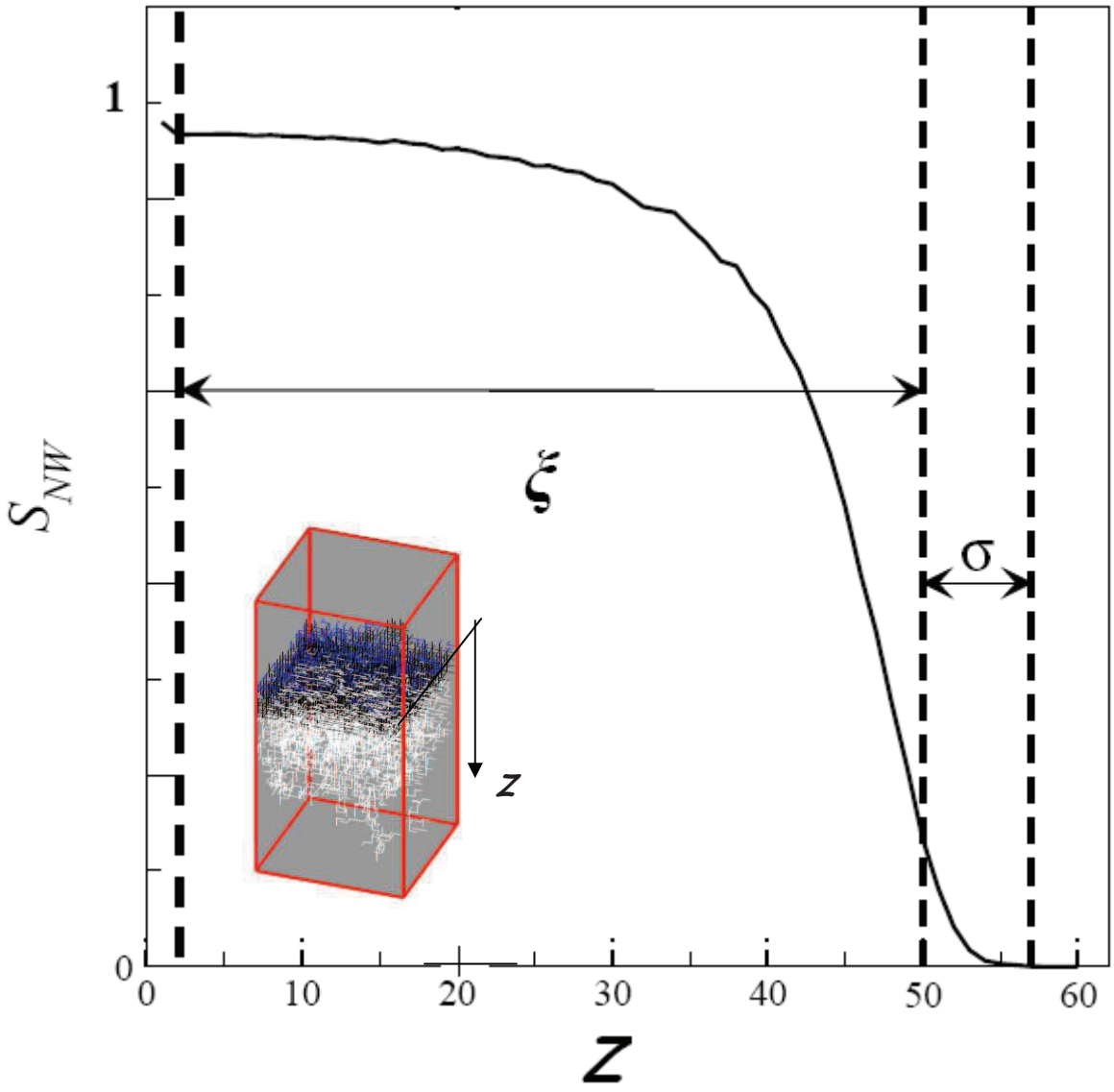

Fig.4

a)

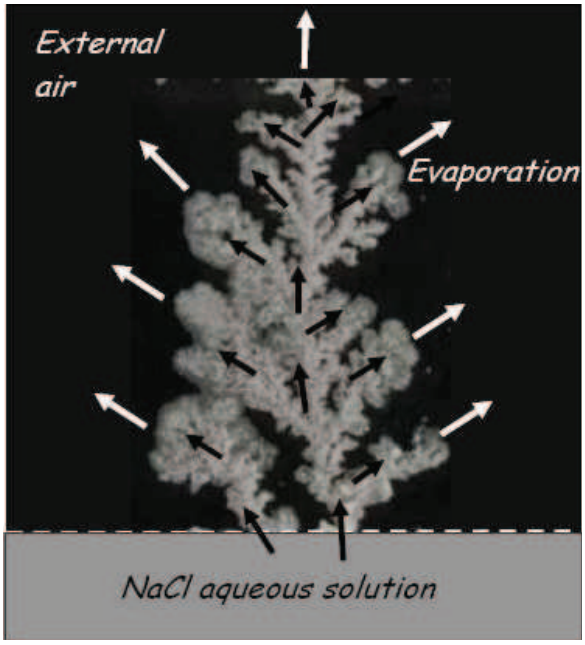

b)

Fig.5

Fig.6

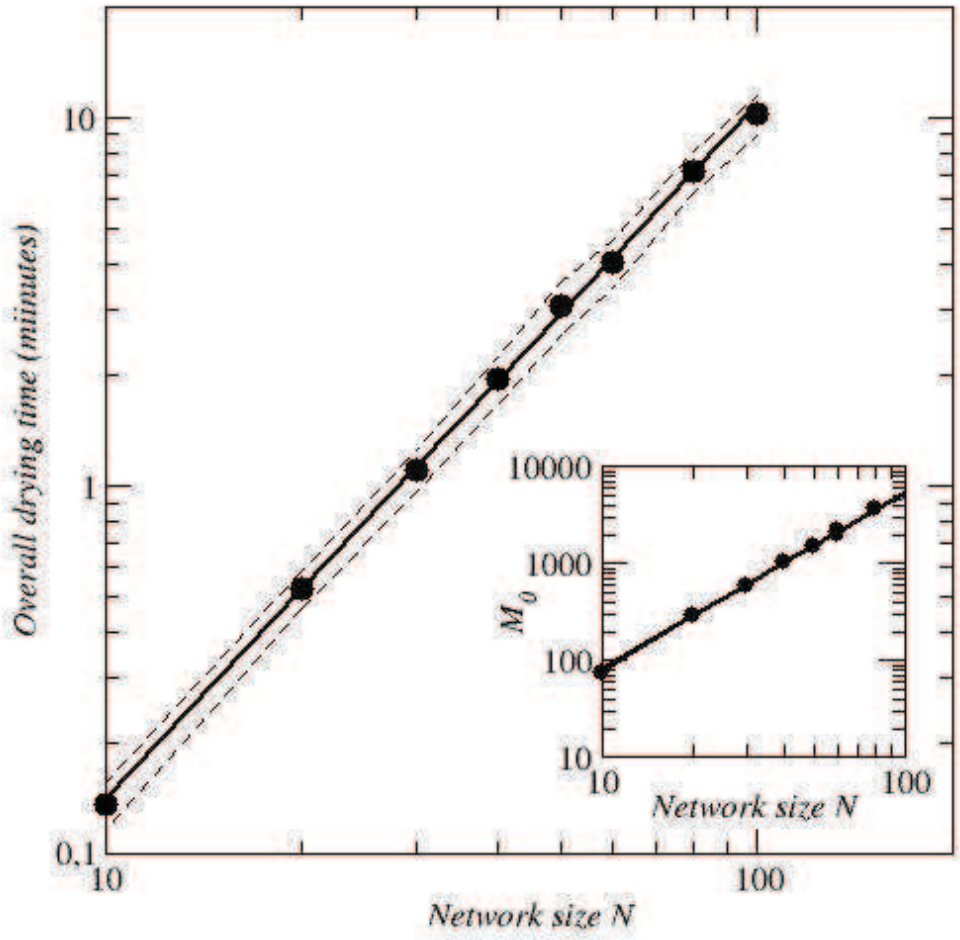
10
1
0,1
10
100
Overall drying time (minutes)
Network size N
10000
1000
100
10
M_0
10
100
Network size N

Fig.7